Available online www.worldscientificnews.com

World Scientific News

An International Scientific Journal

WSN 215 (2026) 36-58 EISSN 2392-2192

# Electro- Hydrodynamic Peristaltic Transport of a Third-Grade Nanofluid Flow in the Presence of Thermal Radiation in an Asymmetric Channel

**Deepa C. Katagi**

Department of Mathematics, Tontadaraya College of Engineering, Mundargi Rd, Panchal Nagar, Kalyan Nagar, Gadag-Betageri, Karnataka 582101, India

*Corresponding author

E-mail: deepackatagi@gmail.com (Deepa C Katagi)

https://doi.org/10.65770/NSTL2501

**ABSTRACT**

This work finds application in micro-fabrication techniques and the chemical industry. This study examines the effects of the magnetic field and electroosmotic repulsion on the peristaltic flow of a third-grade nanofluid in an asymmetric channel. The problem is modelled with the aid of a lubrication approach. The expressions for stream function, velocity, temperature, and species concentration are derived using the Adomian decomposition method. The physical parameters are analyzed and discussed graphically. The significant outcome of this work is to analyze the flow behaviour in both symmetric and asymmetric channels. The results are used to analyze the blood flow through channels, which helps examine the artery blockage treatment and cancer tumour elimination. The velocity profile with the impact of Deborah's number and the electroosmotic parameter is studied for both channels. Validation of obtained results is done in comparison with the previous results.

***Keywords:*** Peristaltic flow, Electroosmosis, Adomian Decomposition Method (ADM), Thermal radiation.

(Received 11 March 2026; Accepted 18 April 2026; Date of Publication 12 May 2026)

## 1. INTRODUCTION

The study of electro-osmosis has received a lot of attention over the past few decades. It is possible to modify peristaltic motion by increasing and decreasing external electric fields. One such example is the incorporation of peristaltic flow using electro-osmosis [1]. Electro-osmotic transport is a prominent topic in microfluidics because of its present applications in healthcare investigations, scientific and biological analysis, cardiac output issues, medicine, and treating ailments like abnormal and sickle cell disease. The investigation of fluid flow is influenced by an external electric field known as electro-osmosis. A charge is generated when an electrolyte solution arrives in contact with the solid interface. When ions are drawn in opposite directions by the surface's electric potential, it leads to the creation of an electron dual layer (EDL). Inducing fluid mobility in an ionic solution with an electric field involves applying an electric charge's net kinetic coupling force. In order to control fluid flow through channels, this phenomenon is used in bio-microfluidics. Electro-osmotic pumps swiftly and easily produce high-pressure liquid flow while being affordable, effective, and lightweight. It is essential to create precise models of electro-osmotic transport using the elastic constants for non-Newtonian and Newtonian fluids and electro-osmotic transit systems in order to comprehend physiological systems and create useful bio-devices. There have been some recent studies on electro-osmotic transfers [2–5].

Due to its usage in engineering, biomedicine, and industry, the magnetic field has attracted much attention. Strong magnetic fields are essential for the operation of electric power generators, electrostatic precipitation, mass spectroscopy (Nuclear Magnetic Resonance) and MRI biomedical equipment (Magnetic Resonance Imaging) which are used to treat diseases. Magnetic fields are also necessary for the separation of metallic materials from non-metallic impurities. The third-grade fluid flow with MHD was investigated by Prasanth and Subba [6]. Hayat and Mehmood [7] explored the impact of slip on the MHD third-grade fluid flow in a planar pipe.

Peristalsis is a succession of muscle relaxation and vessel wall contraction that drives material ahead in fluids via tubes in a wave-like motion without having an interface with the parts of the pump. Peristaltic motion can be witnessed in the transit of food through the stomach, esophagus, and intestinal tract, blood through arteries, veins, and capillaries, urine through the ureter from the kidney to the bladder, and so on. Toxic liquids are transported in nuclear enterprises using the peristaltic phenomena. Additionally, engineers use the finger and roller pumps which run on the principle of peristalsis. Sanitary fluid transportation and other related applications. To circulate blood in the cardiovascular machine during surgery, osmotic motors are also used. The behaviour of a two-dimensional channel peristaltic pump was first examined by Latham [8]. The pulsatile flow of a viscous fluid was explored by Shapiro et al. [9]. Ever since, many initiatives to analyze the peristaltic transport phenomena under various hypotheses have been made (see a few studies [10–15]).

For industrial, medical, and technological applications, the flow of non-Newtonian and Newtonian fluids is preferable. The majority of fluids found in nature are non-Newtonian. Examples are tomato ketchup, blood, mud, honey, and other such fluids. The first researchers to examine the peristaltic flow of non-Newtonian fluids were Raju and Devanathan [16]. Mekheimer [17] investigated blood peristaltic flow in non-uniform channels. These flow issues are challenging to solve because of the highly nonlinear and sophistication of non-Newtonian fluids. A unique subclass of these fluids is termed third-grade fluid, associated with third-order truncation. The fluids of degree three include the fluids of grade three as a subclass. The first mathematical findings on fluids for third grade were reported by Amrouche and Cioranescu [18].

However, the citations only briefly address a few investigations on third-grade fluid [19–20]. The pulsatile flow of a third-grade fluid was then studied by Hayat et al. [21]. Haroun [22] looked at how Deborah's number and phase difference affected grade three fluid pulsatile transport. The third-order fluid flow in a tapered canal was researched by Prakash et al. [23]. Amin [24] studied a third-grade fluid's unsteady thin film fluid flow. Thermal radiation was utilized by Sridhar et al. [25] to describe the impact of mass and heat transfer on the peristalsis of Jeffrey fluid. Few references [26–30] related to the study of MHD, mixed convection, and radiation. Asha and Deepa [31] have investigated peristaltic flow alongside thermal radiation and entropy effects. Additionally, the impact of the MHD in a tapered canal was examined by Asha and Deepa [32]. Several studies on peristaltic flow are listed in the bibliography [33-35].

There is potential for chemical, engineering, and industrial applications of the current work. First, the pulsatile motion of a third-grade nanofluid through an asymmetric channel is examined to determine the effects of electro-osmotic transport, heat radiation, and magnetic field. We discovered that numerous scholars investigated peristaltic flow in various channels throughout the literature survey. However, no research has been done to show how the Adomian decomposition approach can be used on the electro-osmotic flow, radiation, and magnetic field. Finally, the graphs depicting the outcomes of various physical factors on concentration, temperature, velocity, heat-generation coefficient, and electro-osmotic coefficient are provided.

The present study holds potential for chemical, engineering, and industrial applications. First, the electro-osmotic transport, thermal radiation, and magnetic field are investigated in the peristaltic motion of third-grade nanofluid through an asymmetric channel. Throughout the literature review, we found that several researchers examined peristaltic flow in different channels. However, no study has been made to demonstrate the effect of electro-osmotic flow, radiation, and magnetic field in an asymmetric channel by the Adomian decomposition method. Finally, the impact of various physical parameters on temperature, concentration, velocity, heat generation coefficient, and electro-osmotic coefficient were graphically depicted.

## 2. MATHEMATICAL FORMUATION

We address the peristalsis of an immiscible third-order conducting nanofluid. A unified magnetic field is introduced to the flow in a perpendicular direction. By assuming that the fluid has poor electrical conductivity, the magnetic Reynolds number is taken to be modest, and the induced magnetic field is disregarded in favour of the applied magnetic field. The rectangular coordinate system is the one we select $(\tilde{X},\tilde{Y})$ in which the $X$ -axis is located near the channel's centreline and the $Y$ -axis is perpendicular to it. Assume a wave train that is infinite and moves down the channel walls at c velocity. Figure 1 depicts a sketch of the channel.

The wall surfaces' geometry is represented by,

$$h_1\left(X,\tilde{t}\right)=d_1+a_1\cos\left[\frac{2\pi}{\lambda}(X-c\tilde{t})\right]\text{- Upper wall,} \tag{1}$$

$$h_2\left(X,\tilde{t}\right)=-d_2-a_2\cos\left[\frac{2\pi}{\lambda}(X-c\tilde{t})+\phi\right]\text{ - Lower wall,} \tag{2}$$

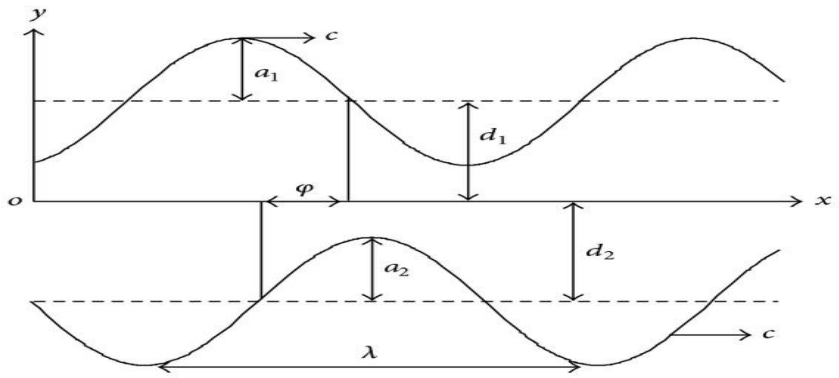


**Figure1.** A sketch of an asymmetric channel.

where $\phi\left(0 \le \phi \le \pi\right)$ is the phase difference, and $a_1$ and $a_2$ are the top wall's and lower wall's respective amplitudes. It is noted that $\phi = \pi$ corresponds to a symmetric channel with in-phase waves and $\phi = 0$ out-of-phase waves. $\tilde{t}$ is the time, $\lambda$ is the wavelength, $d_1$ and $d_2$ is the distance between the upper and lower wall's half-widths. $V$ can be expressed as $V = \left[U\left(X,Y,\tilde{t}\right),V\left(X,Y,\tilde{t}\right),0\right]$ where $U$ and $V$ are the velocities in $X$ and $Y$ direction in the stationary frame. Additionally, $a_1$, $a_2$, $d_1$ and $d_2$ satisfy the relation.

$$a_1^{\,2} + a_2^{\,2} + 2a_1a_2\cos\phi \le (d_1 + d_2)^2.$$

**Electro-hydrodynamics:**

The Poisson Eq. [26] is defined as

$$\nabla^2 \varnothing = -\frac{\rho_e}{\varepsilon}, \tag{3}$$

here $\varepsilon$ is the permittivity of dielectric, $\rho_e$ is the overall density of charges, and $\emptyset$ is the electrical potential.

**Potential distribution:**

The entire charge density is distributed according to the Boltzmann distribution [27].

$$\rho_e = -z_v e\left(n^- - n^+\right). \tag{4}$$

The cations (n+) and anions (n-) are described by Boltzmann's equation.

$$n^{\pm} = n_0 e^{\left(\pm\frac{ezv}{T_{av}k_B}\right)\varnothing}, \tag{5}$$

where the electronic charge is e, the charge balance is $z_v$, the bulk concentration is $n_0$, Boltzmann constant $K_B$ and the average temperature is $T_{av}$.

As a result of Debye-Huckel linearisation [27]. Eq. (3) changes to

$$\frac{d^2\varnothing}{dy^2} = m_e^2\varnothing, \tag{6}$$

The electro-osmotic parameter is $m_e$ and boundary conditions are $\emptyset = 1$ at $y = h_1$ and $\emptyset = -1$ at $y = -h_2$. Eq. (6) yields,

$$\varnothing(y) = \frac{sinh\left[m_e(y+h)\right]}{sinh\left[2hm_e\right]}. \tag{7}$$

The stress tensor model $T$ for a third-order fluid is

$$T = -p\tilde{I} + S, \tag{8}$$

where $\tilde{I}$ is the identity tensor, $p$ is the pressure.

The extra stress tensor $S$ is given by,

$$S = \mu A_1 + \alpha_1 A_2 + \alpha_2 A_2^{\ 2} + \beta_1 A_3 + \beta_2\left(A_2 A_1 + A_1 A_2\right) + \beta_3\left(tr\, A_1^{\ 2}\right)A_1, \tag{9}$$

where the material constants $\mu$, $\alpha_1$, $\alpha_2$, $\beta_1$, $\beta_2$ and $\beta_3$ satisfy the condition $\mu \geq 0, \alpha_1 \geq 0, |\alpha_1 + \alpha_2| \leq \sqrt{24\mu\beta_3}, \beta_1 + \beta_2 = 0, \beta_2 \geq 0$.

The Rivlin- Erickson tensor $A_n$ are expressed by the relation

$$A_1 = \left(gradV\right) + \left(gradV\right)^T, \tag{10}$$

$$A_n = \frac{d}{d\tilde{t}} A_{n-1} + A_{n-1}\left(gradV\right) + \left(gradV\right)^T A_{n-1},\ n \geq 1 \tag{11}$$

The governing Eqs. of mass, momentum, energy, and species concentration are stated as [7].

$$\frac{\partial\tilde{U}}{\partial\tilde{X}} + \frac{\partial\tilde{V}}{\partial\tilde{Y}} = 0, \tag{12}$$

$$\rho\left(\frac{\partial}{\partial\tilde{t}} + \tilde{U}\frac{\partial}{\partial\tilde{X}} + \tilde{V}\frac{\partial}{\partial\tilde{Y}}\right)\tilde{U} = -\frac{\partial\tilde{P}}{\partial\tilde{X}} + \left(\frac{\partial\tilde{S}_{\tilde{X}\tilde{X}}}{\partial\tilde{X}} + \frac{\partial\tilde{S}_{\tilde{X}\tilde{Y}}}{\partial\tilde{Y}}\right) + \rho_e E_x - \sigma B_0^2\tilde{U} + \rho g k\left(\tilde{T} - T_0\right) + \rho g k'\left(\tilde{C} - C_0\right), \tag{13}$$

$$\rho\left(\frac{\partial}{\partial\tilde{t}} + \tilde{U}\frac{\partial}{\partial\tilde{X}} + \tilde{V}\frac{\partial}{\partial\tilde{Y}}\right)\tilde{V} = -\frac{\partial\tilde{P}}{\partial\tilde{Y}} + \left(\frac{\partial\tilde{S}_{\tilde{Y}\tilde{X}}}{\partial\tilde{X}} + \frac{\partial S_{\tilde{Y}\tilde{Y}}}{\partial\tilde{Y}}\right), \tag{14}$$

$$\rho C_P\left(\frac{\partial}{\partial\tilde{t}} + \tilde{U}\frac{\partial}{\partial\tilde{X}} + \tilde{V}\frac{\partial}{\partial\tilde{Y}}\right)\tilde{T} = K\left[\frac{\partial^2}{\partial\tilde{X}^2} + \frac{\partial^2}{\partial\tilde{Y}^2}\right]\tilde{T} + \left(\frac{\partial\tilde{U}}{\partial\tilde{X}}\tilde{S}_{\tilde{X}\tilde{X}} + \frac{\partial\tilde{V}}{\partial\tilde{Y}}\tilde{S}_{\tilde{Y}\tilde{Y}} + \left(\frac{\partial U}{\partial\tilde{X}} + \frac{\partial V}{\partial\tilde{Y}}\right)\tilde{S}_{\tilde{X}\tilde{Y}}\right) - \frac{\partial q_r}{\partial\tilde{Y}}, \tag{15}$$

$$\left(\frac{\partial}{\partial \tilde{t}}+\tilde{U}\frac{\partial}{\partial \tilde{X}}+\tilde{V}\frac{\partial}{\partial \tilde{Y}}\right)\tilde{C}=D_m\left[\frac{\partial^2}{\partial \tilde{X}^2}+\frac{\partial^2}{\partial \tilde{Y}^2}\right]\tilde{C}+\frac{k_t D_m}{T_m}\left[\frac{\partial^2}{\partial \tilde{X}^2}+\frac{\partial^2}{\partial \tilde{Y}^2}\right]\tilde{T}. \tag{16}$$

where $\rho_e$ is the electric charge density, $\rho$ is the fluid density, $E_x$ is the axial electric field, $P$ is the pressure, $\sigma$ is the electrical conductivity, $k$ is the thermal expansion coefficient, g is the acceleration due to gravity, $k'$is the concentration expansion co-efficient., $q_r$ is the radiative heat flux, $k_t$ is the thermal diffusion, $D_m$ is the mass diffusivity, $T_m$ is the average temperature, $\tilde{T}$ and $\tilde{C}$ are the non-dimensional temperature and species concentration, respectively.

**Thermal radiation**

The Rosseland approximation and diffusion approximation can be used to define the radiative flux $q_r$ as

$$q_r=-\frac{4\sigma_1}{3k_1}\frac{\partial \tilde{T}^4}{\partial \tilde{Y}}, \tag{17}$$

$$\frac{\partial q_r}{\partial \tilde{y}}=-\frac{16\sigma_1}{3k_1}\tilde{T}^4\frac{\partial^2 \tilde{T}^4}{\partial \tilde{Y}^2}. \tag{18}$$

By utilising Taylor's series to expand $\tilde{T}^4$ about $T_0$ and ignoring higher-order terms, assuming that temperature variances are small enough to allow for $\tilde{T}^4$ to be represented as

$$\tilde{T}^4 \approx T_0^4+4T_0^3\left(\tilde{T}-T_0\right),$$

$$\tilde{T}^4 \approx -3T_0^4+4T_0^3\tilde{T}, \tag{19}$$

$$\frac{\partial q_r}{\partial \tilde{y}}=-\frac{16\sigma_1}{3k_1}T_0^3\frac{\partial^2 \tilde{T}^4}{\partial \tilde{Y}^2}. \tag{20}$$

Using this in Eq. (15) we have,

$$\rho C_P\left(\frac{\partial}{\partial \tilde{t}}+\tilde{U}\frac{\partial}{\partial \tilde{X}}+\tilde{V}\frac{\partial}{\partial \tilde{Y}}\right)\tilde{T}=K\left[\frac{\partial^2}{\partial \tilde{X}^2}+\frac{\partial^2}{\partial \tilde{Y}^2}\right]\tilde{T}+\left(\frac{\partial \tilde{U}}{\partial \tilde{X}}\tilde{S}_{\tilde{X}\tilde{X}}+\frac{\partial \tilde{V}}{\partial \tilde{Y}}\tilde{S}_{\tilde{Y}\tilde{Y}}+\left(\frac{\partial U}{\partial \tilde{X}}+\frac{\partial V}{\partial \tilde{Y}}\right)\tilde{S}_{\tilde{X}\tilde{Y}}\right)+\frac{16\sigma_1}{3k_1}T_0^3\frac{\partial^2 \tilde{T}^4}{\partial \tilde{Y}^2}. \tag{21}$$

We analyze the following transformations between the steady stationary frame $(\tilde{X},\tilde{Y})$ and the unsteady moving frame $(\tilde{x},\tilde{y})$ [29],

$$\tilde{x}=\tilde{X}-c\tilde{t},\ \tilde{y}=\tilde{Y},\ \tilde{v}(\tilde{x},\tilde{y})=\tilde{V}\left(\tilde{X},Y\tilde{t}\right),\ \tilde{u}(\tilde{x},\tilde{y})=\tilde{U}\left(\tilde{X},Y\tilde{t}\right)-c,\ \tilde{t}(\tilde{x},\tilde{y})=\tilde{T}\left(\tilde{X},\tilde{Y},\tilde{t}\right)\ \tilde{p}(\tilde{x},\tilde{y})=\tilde{P}\left(\tilde{X},\tilde{Y},\tilde{t}\right),. \tag{22}$$

Employing the transformations in Eqs. (12) to (14), (16) and (21) we implement the dimensionless quantities listed below;

$$x=\frac{2\pi\tilde{x}}{\lambda},y=\frac{\tilde{y}}{a},t=\frac{2\pi c\tilde{t}}{\lambda},u=\frac{\bar{u}}{c},v=\frac{\bar{v}}{c},p=\frac{2\pi a^2}{\lambda c\mu}\tilde{p},\alpha=\frac{2\pi a}{\lambda},h=\frac{\tilde{h}}{a},P_e=\frac{C\lambda}{D},m_e=\frac{a}{\lambda D},$$

$$n=\frac{\tilde{n}}{n_0},\check{n}=\frac{b}{a},\theta=\frac{\tilde{T}-T_0}{T_0},\phi=\frac{\tilde{C}-C_0}{C_0},\lambda_D=\frac{1}{ez_v}\sqrt{\frac{T_0\check{n}K_B}{2n_0}},E_c=\frac{c^2}{c_pT_0},\varnothing=\frac{ez_v}{T_{av}K_B}\tilde{\varnothing},U_{hs}=-\frac{E_x\check{n}}{c\mu}$$

$$S=\frac{a}{c\mu}\tilde{S},\lambda_1=\frac{a_1c}{a\mu},\lambda_2=\frac{a_2c}{a\mu},\gamma_1=\frac{\beta_1c^2}{\alpha^2\mu},\gamma_2=\frac{\beta_2c^2}{\alpha^2\mu},\gamma_3=\frac{\beta_3c^2}{\alpha^2\mu},\Gamma=\gamma_3+\gamma_2,S_c=\frac{\mu}{\rho D_m},$$

$$S_r=\frac{\rho D_mK_TT_0}{\mu T_mC_0},G_r=\frac{\rho gB_TT_0a^2}{c\mu},G_c=\frac{\rho gB_cC_0a^2}{c\mu},R_n=\frac{16\sigma_1}{3c_p\mu k_1}T_0^3,M^2=\frac{\sigma a^2B_0^2}{\mu},\psi=\frac{\tilde{\psi}}{ca},u=\frac{\partial\psi}{\partial y},$$

$$v=-\alpha\frac{\partial\psi}{\partial x},Re=\frac{\rho ca}{\mu},P_r=\frac{\mu c_p}{k},B_r=E_cP_r,F=\frac{\tilde{q}}{ca},\Theta=\frac{\tilde{Q}}{ca}. \tag{23}$$

In view of (23), Eqs. (13)-(15) and (21) become,

$$Re\alpha\left[\frac{\partial\psi}{\partial y}\frac{\partial}{\partial x}-\frac{\partial\psi}{\partial y}\frac{\partial}{\partial y}\right]\frac{\partial\psi}{\partial y}=-\frac{\partial p}{\partial x}+\left(\alpha\frac{\partial S_{xx}}{\partial x}+\frac{\partial S_{xy}}{\partial y}\right)+m_e^2U_{hs}\varnothing-M^2\left(\frac{\partial\psi}{\partial y}+1\right)+G_r\theta+G\phi_c, \tag{24}$$

$$-Re\alpha^3\left[\frac{\partial\psi}{\partial y}\frac{\partial}{\partial x}-\frac{\partial\psi}{\partial y}\frac{\partial}{\partial y}\right]\frac{\partial\psi}{\partial x}=-\frac{\partial P}{\partial y}+\alpha\left(\alpha\frac{\partial S_{xx}}{\partial x}+\frac{\partial S_{xy}}{\partial y}\right), \tag{25}$$

$$Re\,\alpha\left[\frac{\partial\psi}{\partial y}\frac{\partial}{\partial x}-\frac{\partial\psi}{\partial y}\frac{\partial}{\partial y}\right]\theta=\frac{1}{P_r}\left(\alpha^2\frac{\partial^2}{\partial x^2}+\frac{\partial^2}{\partial y^2}\right)\theta+E_c\left[\alpha^2\frac{\partial}{\partial x}\left(\frac{\partial\psi}{\partial x}\right)S_{xx}-\alpha\frac{\partial}{\partial y}\left(\frac{\partial\psi}{\partial x}\right)S_{yy}+\left(\frac{\partial^2\psi}{\partial y^2}-\alpha^2\frac{\partial^2\psi}{\partial x^2}\right)S_{xy}\right]+ R_n\frac{\partial^2\theta}{\partial y^2}, \tag{26}$$

$$Re\alpha\left[\frac{\partial\psi}{\partial y}\frac{\partial}{\partial x}-\frac{\partial\psi}{\partial y}\frac{\partial}{\partial y}\right]\Omega=\frac{1}{S_C}\left(\alpha^2\frac{\partial^2}{\partial x^2}+\frac{\partial^2}{\partial y^2}\right)\Omega+S_r\left(\alpha^2\frac{\partial^2}{\partial x^2}+\frac{\partial^2}{\partial y^2}\right)\theta. \tag{27}$$

Utilising the low Reynolds number and long wavelength approximations for Eqs. (24)-(27) and omitting higher order terms of the result, we arrive at

$$\frac{\partial p}{\partial x}=\frac{\partial\left(S_{xy}\right)}{\partial x}+m_e^2U_{hs}\varnothing-M^2\left(\frac{\partial\psi}{\partial y}+1\right)+G_r\theta+G_c\phi=0, \tag{28}$$

$$\frac{\partial p}{\partial y} = 0, \tag{29}$$

$$\frac{\partial^2 \theta}{\partial y^2}\left(1 + R_n P_r\right) + B_r\left[S_{xy}\right]\frac{\partial^2 \psi}{\partial y^2} = 0, \tag{30}$$

$$\frac{\partial^2 \Omega}{\partial y^2} + S_C S_r\left(\frac{\partial^2 \theta}{\partial y^2}\right) = 0. \tag{31}$$

Omitting pressure from Eqs. (28) and (29), we obtain

$$\frac{\partial^2\left(S_{xy}\right)}{\partial y^2} + m_e^2 U_{hs}\phi - M^2\left(\frac{\partial^2 \psi}{\partial y^2}\right) + G_r\frac{\partial \theta}{\partial y} + G_c\frac{\partial \phi}{\partial y} = 0, \tag{32}$$

where $S_{xy} = \frac{\partial^2 \psi}{\partial y^2} + 2\Gamma\left(\frac{\partial^2 \psi}{\partial y^2}\right)^3$.

The non-dimensional boundary conditions are,

$$\begin{aligned} &\psi = \frac{F}{2}, \frac{\partial \psi}{\partial y} = 0, \theta = 0, \phi = 0, \quad at\ y = h_1 \\ &\psi = -\frac{F}{2}, \frac{\partial \psi}{\partial y} = 0, \theta = 1, \phi = 1, \quad at\ y = h_2 \end{aligned} \tag{33}$$

The non-dimensional mean flow rate F in the moving frame and fixed frame are related by,

$$\Theta = \mathrm{F} + 1, \tag{34}$$

where, $F = \int_{-h_1}^{h_2} \frac{\partial \psi}{\partial y} dy = \psi\left[h_1(x)\right] + \psi\left[-h_2(x)\right]$.

The non-dimensional heat transfer co-efficient is given by,

$$Z = h_x\left|\frac{\partial \theta}{\partial y}\right|. \tag{35}$$

## 3. METHOD OF SOLUTION

The nonlinear system of the preceding Eqs. (28)–(31) with the boundary conditions (33) are solved by employing the Adomian decomposition method. Double integration of Eq. (31) yields

$$\theta = c_1 e^{s_1 y} + c_2 e^{-s_1 y}, \tag{36}$$

Using the above Eq. (36) in Eq. (30), we get,

$$\Omega = \frac{-(S_c S_r)\left(e^{-s_1 h_1} e^{s_1} y + e^{s_1 h_1} e^{-s_1 y}\right)}{\left(e^{s_1 h_1} e^{s_1 h_2} - e^{s_1 h_1} e^{-s_1 h_2}\right)} - c_3 y - c_4 , \tag{37}$$

where $s_1 = \sqrt{\frac{QP_r}{(1+N_r)}}$.

Utilising the suitable boundary conditions of Eq. (33), we obtain,

$$c_1 = \frac{e^{s_1 h_2}}{\left(e^{-s_1(h_1-h_2)} - e^{s_1(h_1-h_2)}\right)e^{s_1(h_1+h_2)}}, \text{ and } c_2 = \frac{e^{s_1 h_1}}{\left(e^{-s_1(h_1-h_2)} - e^{s_1(h_1-h_2)}\right)},$$

$$c_3 = -\frac{1}{(h_2-h_1)} - \frac{(S_c\, S_r)}{\left(e^{s_1 h_1} e^{s_1 h_2} - e^{s_1 h_1} e^{-s_1 h_2}\right)(h_2-h_1)}\left[\frac{e^{-s_1 h_1} e^{s_1 h_2} + e^{s_1 h_1} e^{-s_1 h_2}}{{h_2}^2} - \frac{e^{-s_1 h_1} e^{s_1 h_1} + e^{s_1 h_1} e^{-s_1 h_1}}{{h_1}^2}\right],$$

$$c_4 = \frac{(S_c\, S_r)\left(e^{-s_1 h_1} e^{s_1 h_1} + e^{s_1 h_1} e^{-s_1 h_1}\right)}{\left(e^{s_1 h_1} e^{s_1 h_2} - e^{s_1 h_1} e^{-s_1 h_2}\right)} + \frac{h_1}{(h_2-h_1)} + \frac{(S_c\, S_r)}{\left(e^{s_1 h_1} e^{s_1 h_2} - e^{s_1 h_1} e^{-s_1 h_2}\right)(h_2-h_1)}$$
$$\left[\frac{e^{-s_1 h_1} e^{s_1 h_2} + e^{s_1 h_1} e^{-s_1 h_2}}{{h_2}^2} - \frac{e^{-s_1 h_1} e^{s_1 h_1} + e^{s_1 h_1} e^{-s_1 h_1}}{{h_1}^2}\right].$$

The Adomian Decomposition Method (ADM) is implemented to solve Eq. (28) in the following manner;

$$L_{yyy}[\psi] - n^2[\psi_y] = \frac{\partial p}{\partial x}\Big/ 2\Gamma + n^2 - \frac{\partial^2}{\partial y^2}[\psi_{yy}]^3 - \frac{G_t}{2\Gamma}\theta - \frac{G_c}{2\Gamma}\phi , \tag{38}$$

where $n^2 = M^2$.

The inverse operator $L_{yyy}^{-1} = \iiint [.]dydydy$ can be used to write Eq. (5.27) as,

$$\psi = \frac{1}{2\Gamma}\left(c_1 + c_2 y + c_3 \frac{y^2}{2!}\right) + \frac{1}{2\Gamma} L_{yyy}^{-1}\left[\frac{\partial p}{\partial x} + n^2\right] + \frac{1}{2\Gamma} L_{yyy}^{-1}\left[n^2 \psi_y\right] - L_{yyy}^{-1}\left[\frac{\partial^2}{\partial y^2}[\psi_{yy}]^3\right]$$
$$- \frac{Gt}{2\Gamma} L_{yyy}^{-1}[\theta] - \frac{Gc}{2\Gamma} L_{yyy}^{-1}[\phi]. \tag{39}$$

We now decompose $\psi$ as $\psi = \sum_{n=0}^{\infty} \psi_n$, where $n \geq 0$ (40)

$$\psi_0 = \frac{1}{2\Gamma}\left(A_1 + A_2 y + A_3 \frac{y^2}{2!}\right) + \frac{1}{2\Gamma}\left\{\left(\frac{\partial p}{\partial x} + n^2\right) - Gtc_3 + Gc\left(SrSc + \frac{N_t}{N_b}\right)c_3 + Gcc_2\right\}\frac{y^3}{3!}$$
$$+ \frac{1}{2\Gamma}\left\{Gcc_4\left(SrSc + \frac{N_t}{N_b}\right) - Gtc_4\right\}\frac{e^{Cy}}{y^3} + \frac{1}{2\Gamma} Gcc_1 \frac{y^4}{4!}, \tag{41}$$

$$\psi_{n+1} = \iiint \left[ \frac{n^2}{2\Gamma} (\psi_n)_y \right] dydydy - \iiint \frac{\partial^2}{\partial y^2} \left[ (\psi_n)_{yy} \right]^3. \text{ where } n \geq 0$$

Therefore,

$$\psi_1 = k^2 \left[ A_2 \frac{y^3}{3!} + A_3 \frac{y^4}{4!} + \left\{ \left( \frac{\partial p}{\partial x} + n^2 \right) - Gtc_3 + Gc \left( SrSc + \frac{N_t}{N_b} \right) c_3 + Gcc_2 \right\} \frac{y^5}{5!} + \left\{ Gcc_4 \left( SrSc + \frac{N_t}{N_b} \right) - Gtc_4 \right\} \frac{e^{Cy}}{y^3} + Gcc_1 \frac{y^6}{6!} \right],$$

$$\psi_2 = k^4 \left[ A_2 \frac{y^5}{5!} + A_3 \frac{y^6}{6!} + \left\{ \left( \frac{\partial p}{\partial x} + n^2 \right) - Gtc_3 + Gc \left( SrSc + \frac{N_t}{N_b} \right) c_3 + Gcc_2 \right\} \frac{y^7}{7!} + \left\{ Gcc_4 \left( SrSc + \frac{N_t}{N_b} \right) - Gtc_4 \right\} \frac{e^{Cy}}{y^7} + Gcc_1 \frac{y^8}{8!} \right],$$

$$\psi_n = k^{2n} \left[ A_2 \frac{y^{2n+1}}{(2n+1)!} + A_3 \frac{y^{2n+2}}{(2n+2)!} + \left\{ \left( \frac{\partial p}{\partial x} + n^2 \right) - Gtc_3 + Gc \left( SrSc + \frac{N_t}{N_b} \right) c_3 + Gcc_2 \right\} \frac{y^{2n+3}}{(2n+3)!} + \left\{ Gcc_4 \left( SrSc + \frac{N_t}{N_b} \right) - Gtc_4 \right\} \frac{e^{Cy}}{y^{2n+3}} + Gcc_1 \frac{y^{2n+4}}{(2n+4)!} \right].$$

where $k = \left( \frac{n}{2\Gamma} \right)^2$.

The analytical solution of $\psi$ can be expressed as follows, according to Eq. (40)

$$\psi = \frac{A_1}{2\Gamma} + \left[ \frac{A_2}{k} \sinh(ky) + \frac{A_3}{k^2} (\cosh(ky) - 1) \left\{ \left( \frac{\partial p}{\partial x} + n^2 \right) - Gtc_3 + Gcc_3 \left( SrSc + \frac{N_t}{N_b} \right) + Gcc_2 \right\} \frac{1}{k^3} (\sinh(ky) - ky) + \left\{ Gcc_4 \left( SrSc + \frac{N_t}{N_b} \right) - Gtc_4 \right\} \frac{e^{Cy}}{Ck^2} + \frac{Gcc_1}{k^4} \left( \cosh(ky) - 1 - \frac{(ky)^2}{2!} \right) \right],$$

which can be simplified as,

$$\psi = F_1 + F_2 \sinh(ky) + F_3 \cosh(ky) + e^{Cy} \cosh(ky). \tag{42}$$

where

$$F_1 = \frac{F}{4\Gamma} - \left[ \frac{A_2}{k} \sinh(kh_1) + \frac{A_3}{k^2} (\cosh(kh_1) - 1) \left\{ \left( \frac{\partial p}{\partial x} + n^2 \right) - Gtc_3 + Gcc_3 \left( SrSc + \frac{N_t}{N_b} \right) + Gcc_2 \right\} \frac{1}{k^3} (\sinh(kh_1) - kh_1) + \left\{ Gcc_4 \left( SrSc + \frac{N_t}{N_b} \right) - Gtc_4 \right\} \frac{e^{Ch_1}}{Ck^2} + \frac{Gcc_1}{k^4} \left( \cosh(kh_1) - 1 - \frac{(kh_1)^2}{2!} \right) \right],$$

$$F_2 = \frac{-\tanh(kh_2)}{\sinh[k(h_1+h_2)]}+\left[\left\{\left(\frac{\partial p}{\partial x}+n^2\right)-Gtc_3+Gcc_3\left(SrSc+\frac{N_t}{N_b}\right)+Gcc_2\right\}\left(\frac{\cosh(kh_1-1)\cosh(kh_2)}{k^2}\right.\right.$$
$$\left.-\frac{\cosh(kh_1-1)\cosh(kh_2)}{k^2}\right)+\left\{Gcc_4\left(SrSc+\frac{N_t}{N_b}\right)-Gtc_4\right\}\left(\frac{e^{Ch_1}\cosh(kh_2)}{k^2}-\frac{e^{Ch_2}\cosh(kh_1)}{k^2}\right)+$$
$$\frac{Gcc_1}{k^3}\left(\{\sinh(kh_2)+kh_2\}\cosh(kh_1)-\{\sinh(kh_1)+kh_1\}\cosh(kh_2)\right)+\left\{\left(\frac{\partial p}{\partial x}+n^2\right)-Gtc_3+\right.$$
$$\left.Gcc_3\left(SrSc+\frac{N_t}{N_b}\right)+Gcc_2\right\}\frac{\cosh(kh_2-1)\cosh(kh_1)}{k^2}-\frac{Gcc_1}{k^3}\{\sinh(kh_2)+kh_2\}\cosh(kh_1),$$

$$F_3 = \frac{-k}{\sinh[k(h_1+h_2)]}\left\{\left(\frac{\partial p}{\partial x}+n^2\right)-Gtc_3+Gcc_3\left(SrSc+\frac{N_t}{N_b}\right)+Gcc_2\right\}\left(\frac{\cosh(kh_1-1)\cosh(kh_2)}{k^2}\right.$$
$$\left.-\frac{\cosh(kh_2-1)\cosh(kh_1)}{k^2}\right)+\left\{Gcc_4\left(SrSc+\frac{N_t}{N_b}\right)-Gtc_4\right\}\left(\frac{e^{Ch_1}\cosh(kh_2)}{k^2}-\frac{e^{Ch_2}\cosh(kh_1)}{k^2}\right)+$$
$$\frac{Gcc_1}{k^3}\left(\{\sinh(kh_2)+kh_2\}\cosh(kh_1)-\{\sinh(kh_1)+kh_1\}\cosh(kh_2)\right).$$

The velocity expression is provided by

$$u = A_2\cosh(ky)-\frac{A_3}{k}\sinh(ky)+\left\{\left(\frac{\partial p}{\partial x}+n^2\right)-Gtc_3+Gcc_3\left(SrSc+\frac{N_t}{N_b}\right)+Gcc_2\right\}\frac{\cosh(ky-1)}{k^2}+$$
$$\left\{Gcc_4\left(SrSc+\frac{N_t}{N_b}\right)-Gtc_4\right\}\frac{e^{Cy}}{k^2}-\frac{Gcc_1}{k^3}\{\sinh(ky)+ky\}. \qquad (43)$$

## 4. RESULTS AND DISCUSSION

The impacts of various physical parameters are discussed, such as magnetic field parameter M, Grashoff number $G_r$, Species concentration Grashoff number $G_c$, Deborah number Γ, electro-osmotic parameter $m_e$, Schmidt number $S_c$, Soret number $S_r$, Brinkmann number $B_r$ and thermal radiation parameter $R_n$ on temperature, velocity, concentration, and heat transfer coefficient are discussed in this section.

### 4.1. Effect of axial velocity for (a) magnetic field parameter M, (b) Grashoff number $G_r$, (c) Species concentration Grashoff number $G_c$, (d) Deborah number Γ, (e) electro-osmotic parameter $m_e$ (For asymmetric channel)

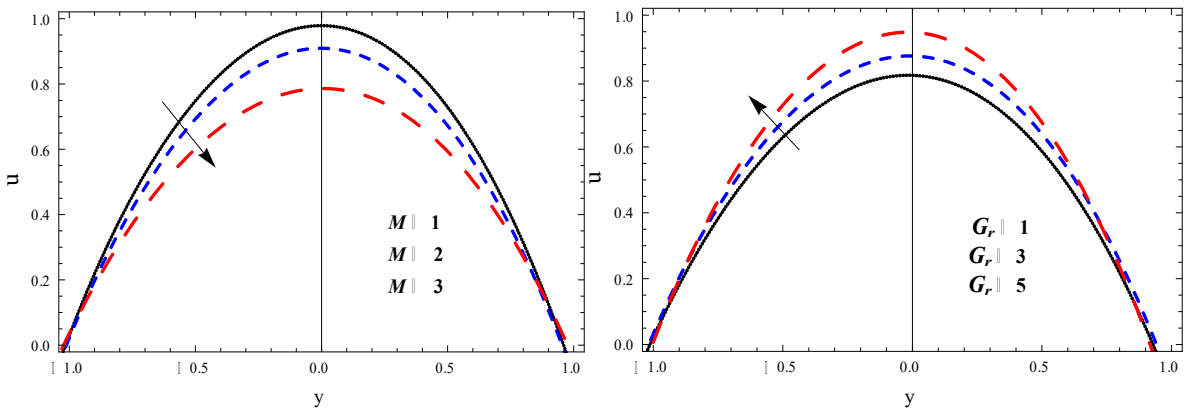

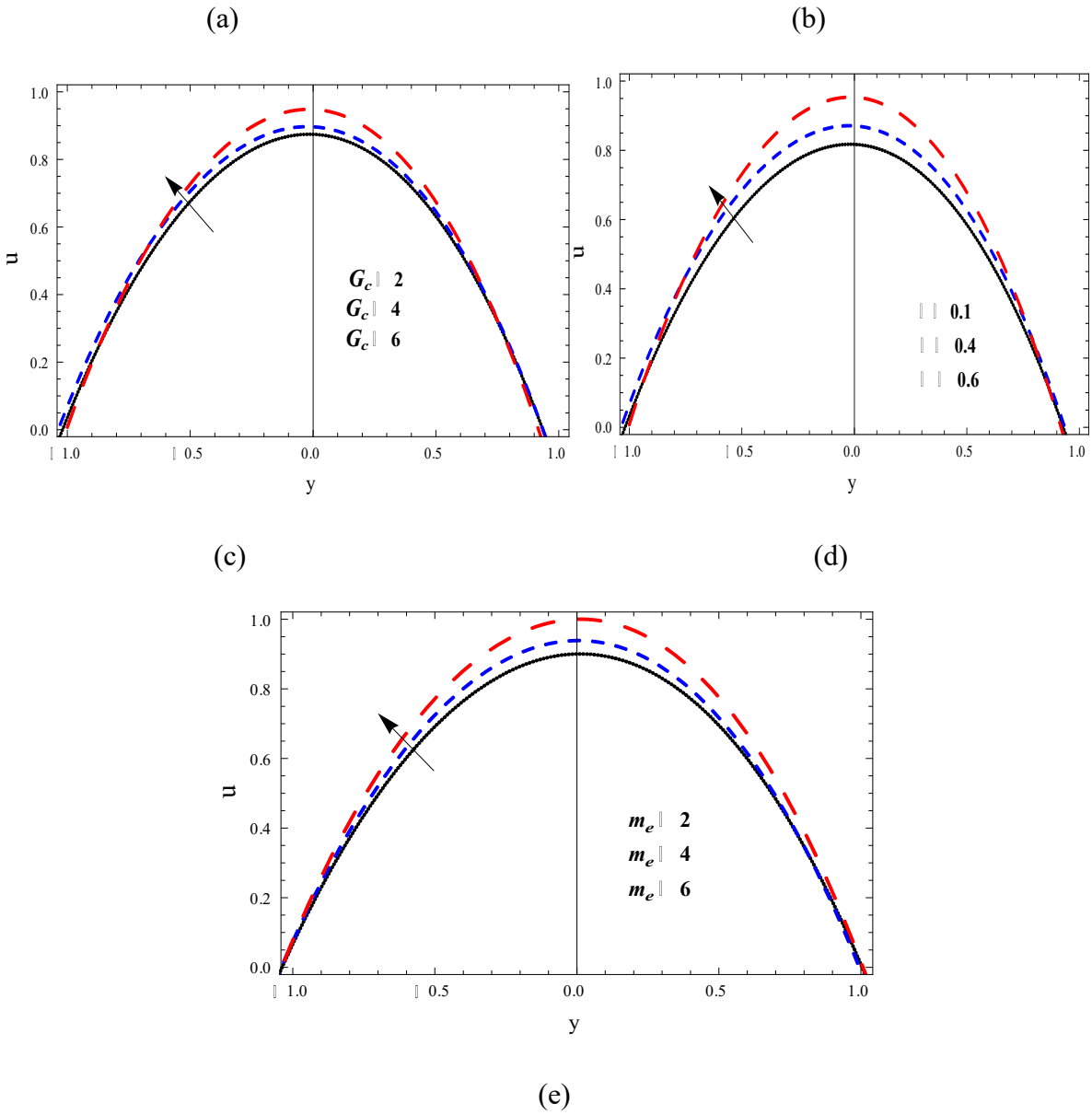


**Figure 2.** Velocity profile ($u$) for (a) M(b) $G_r$ (c) $G_c$ (d) Γ (e) $m_e$, while other parameters are $x = 0.2, U = -2, m_e = 2, B_r = 2, \Gamma = 0.01, M = G_r = S_c = S_r = R_n = P_r = 1, G_c = 0.2, \Theta = 1.8.$

Figure 2 describes the velocity profile for various parameters such as magnetic field parameter $M(1 \leq M \leq 3)$, the temperature Grashoff number $G_r(1 \leq G_r \leq 5)$, the concentration Grashoff number $G_c(2 \leq G_C \leq 6)$, Deborah number Γ $(0.1 \leq \Gamma \leq 0.6)$ and electro-osmotic parameter $m_e$ $(2 \leq m_e \leq 6)$. In figure 2 (a), it can be observed that a higher value of $M$ decreases the velocity. This is because of the Lorentz forces. Figure 2 (b) depicts that an increase in $G_r$ enhances velocity. This is because as velocity increases, the buoyant forces increase. Figure 2 (c) shows a similar effect, where as $G_c$ grows, the left wall velocity and right wall velocity increases. Figure 2 (d) demonstrates that as Γ rises, the velocity u increases at the centre of the channel and near the channel walls. In Figure 2 (e), we observe that the magnitude of $u$ is enhanced near the walls of the channel as $m_e$ increases. The reason for this is as $m_e$ increases, the effect of the electric field increases which accelerates the fluid particles and hence enhances the velocity.

**4.1.1. Effect of axial velocity for (a) Deborah number Γ (b) electro-osmotic parameter $m_e$ (for symmetric channel)**

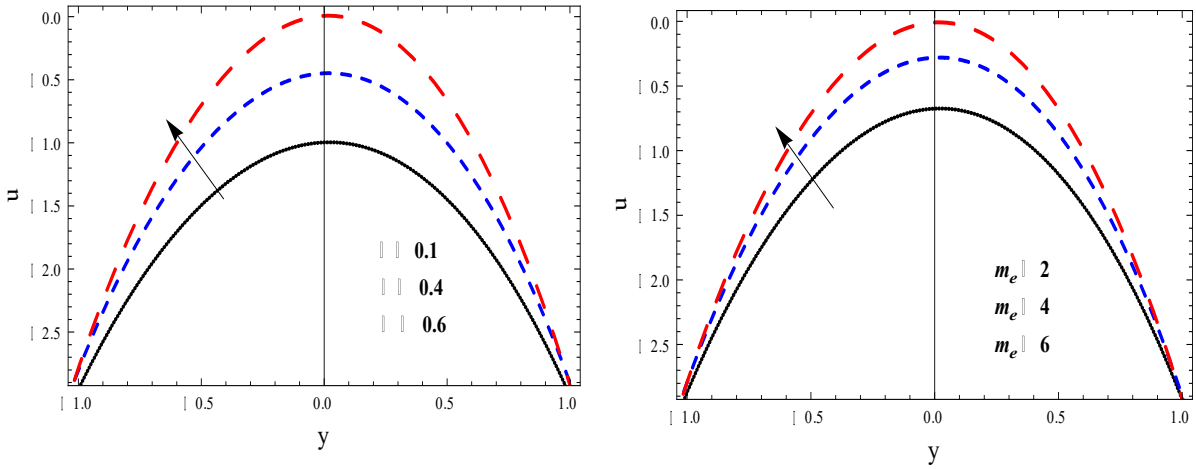


(a) (b)

**Figure 2.1.** Velocity profile ($u$) for (a) M(b) $G_r$ (c) $G_c$ (d) Γ (e) $m_e$, while other parameters are $x = 0.2, U = -2, m_e = 2, B_r = 2, \Gamma = 0.01, M = G_r = S_c = S_r = R_n = P_r = 1, G_c = 0.2, \Theta = 1.8$

Figures 2.1.(a) and (b) depict the velocity profile for Deborah number Γ and electro-osmotic parameter $m_e$ (for symmetric channel). It is observed that both Deborah number Γ and electro-osmotic parameter $m_e$ enhance the velocity profile. Similar results are obtained in Fig. 2(d) and (e) for a asymmetric channel. It is observed from fig. 2(d) and 2.1(a) that, as the electro-osmotic parameter $m_e$ increases from $m_e = 2, 4, 6$, the magnitude of velocity for an asymmetric channel increases by 25% approximately (see fig. 2(d)) whereas the magnitude of velocity for a symmetric channel increases by 95% approximately (see fig. 2.1 (a)). Similarly, it is observed from fig. 2(e) and 2.1(b) that as Deborah number Γ increases, the magnitude of velocity for an asymmetric channel increases by 20% approximately (see fig. 2(e)) whereas the magnitude of velocity for a symmetric channel increases by 63% approximately (see fig. 2.1 (b)).

**4.2. Effect of Temperature for different parameters, such as Brinkman number $B_r$, electro-osmotic parameter $m_e$, Deborah number Γ and thermal radiation parameter $R_n$.**

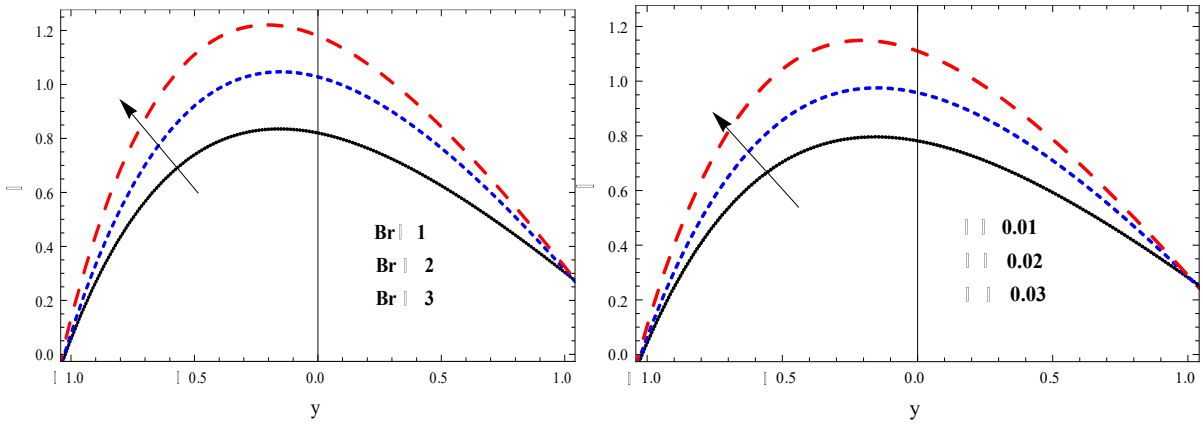


(a) (b)

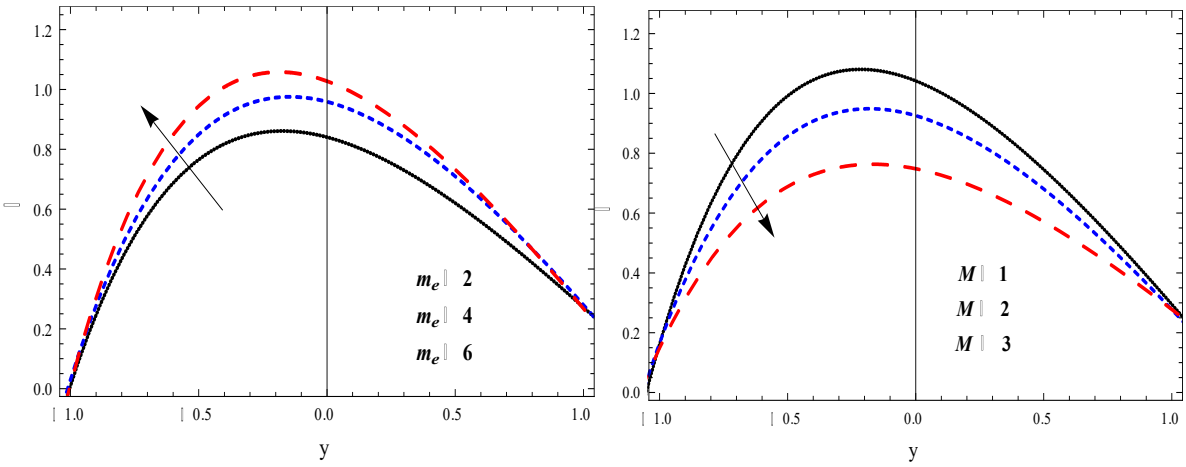


(c) (d)

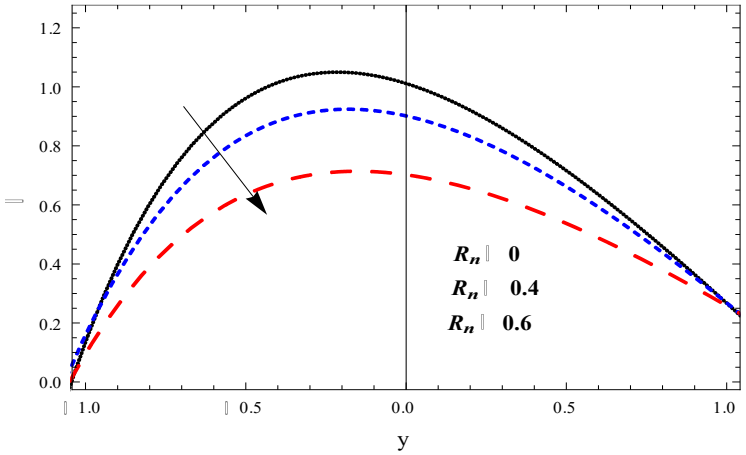


(e)

**Figure 3.** Temperature ($\theta$) for (a) $B_r$ (b) $\Gamma$ (c) $m_e$ (d) M (e)$\gamma$ (f)$R_n$, while other parameters are $x = 0.2, U = -2, m_e = 2, B_r = 2, \Gamma = 0.01, M = G_r = S_c = S_r = R_n = P_r = 1, G_c = 0.2, \Theta = 1.8$

Figure 3 encases the temperature profile $\theta$ for different parameters such as Brinkman number $B_r$ $(1 \leq B_r \leq 5)$, electro-osmotic parameter $m_e (2 \leq m_e \leq 6)$, magnetic field parameter $M$ $(1 \leq M \leq 3)$, Deborah number $\Gamma$ $(0.1 \leq \Gamma \leq 0.6)$ and thermal radiation parameter $R_n (0.0 \leq R_n \leq 0.6)$ respectively. Figure 3(a) shows how an increase in $B_r$ enhances fluid temperature because it reflects viscous dissipation or the conversion of kinetic energy to internal energy in response to viscosity. Figure 3(b) reveals that the temperature profile $\theta$ is enhanced as $\Gamma$ increases. This is because Deborah number characterizes the fluidity of materials under certain flow conditions. As Deborah number enhances, there is a deformity in the fuid particles which enhances the temperature. Figure 3(c) shows that as $\theta$ increases, the fluid particles get charged and leads to higher values of $m_e$, whereas the temperature $\theta$ reduces for higher $M$ as seen in Figure 3(d). Figure 3(e) depicts that the temperature is decelerated by enhancing $R_n$.

**4.3. Concentration profile for various parameters such as Deborah number Γ, electro-osmotic parameter $m_e$, Schmidt number $S_c$, Soret number $S_r$, Brinkmann number $B_r$**

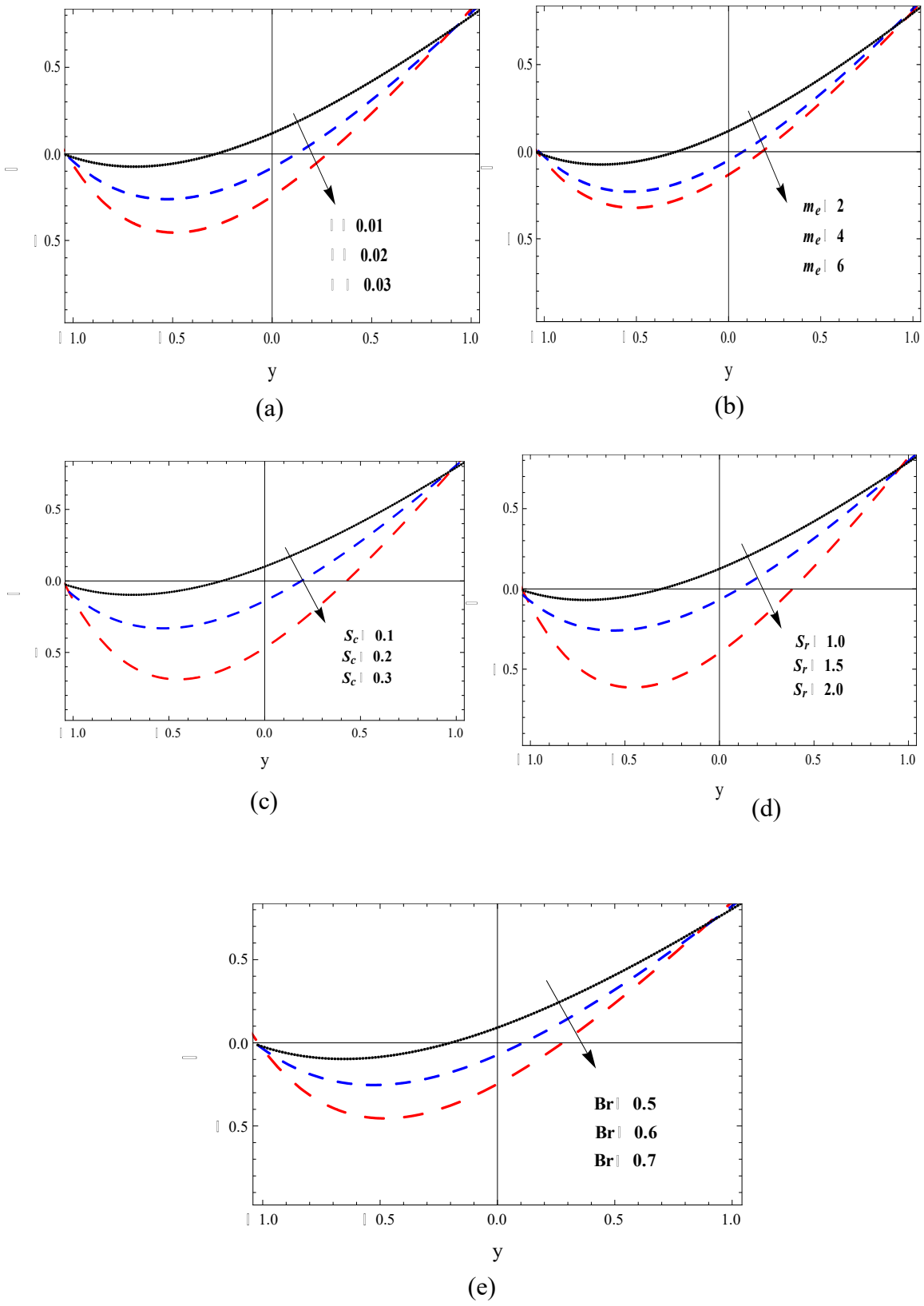


**Figure 4.** Concentration ($\phi$) for (a) $\Gamma$ (b) $m_e$ (c) $S_r$ (d) $S_c$ (e) $B_r$, while other parameters are $x = 0.2, U = -2, m_e = 2, B_r = 2, \Gamma = 0.01, M = G_r = S_c = S_r = R_n = P_r = 1, G_c = 0.2, \Theta = 1.8$

Figure 4 explains the concentration profile for diverse parameters such as Deborah number Γ $(0.1 \leq \Gamma \leq 0.6)$, electro-osmotic parameter $m_e$ $(2 \leq m_e \leq 6)$, Schmidt number $S_c$ $(0.1 \leq S_c \leq 0.3)$, Soret number $S_r$ $(1 \leq S_r \leq 2)$ and Brinkmann number $B_r$ $(0.5 \leq B_r \leq .7)$. Figure 4(a) showss that higher values of Γ decrease $\emptyset$. It is because of the deformity caused for higher values Γ . Figure 4(b) manifests that $\emptyset$ reduces for higher values of $m_e$. As $m_e$ increases there is a migration of the fluid molecules which reduces the concentration. Figure 4(c) intimates that $\emptyset$ is decelerated for more values of $S_c$. Since Schmidts number is the ratio of kinematic viscosity to mass diffusivity, As $S_c$ increases, there is a decrease in the mass diffusivity, which reduces the concentration. A similar result is obtained in Figure 4(d) for different values of $S_r$. Figure 4(e) expresses that $\emptyset$ decreases for higher values of $B_r$.This behaviour is due the slower the conduction of heat produced by viscous dissipation with an increase in $B_r$ and hence the lowers the concentration profile.

**4.4. Impact of Heat transfer co-efficient for different parameters such as Deborah number Γ, magnetic field parameter M, thermal radiation parameter $R_n$, electro-osmotic parameter $m_e$ and Brinkmann number $B_r$.**

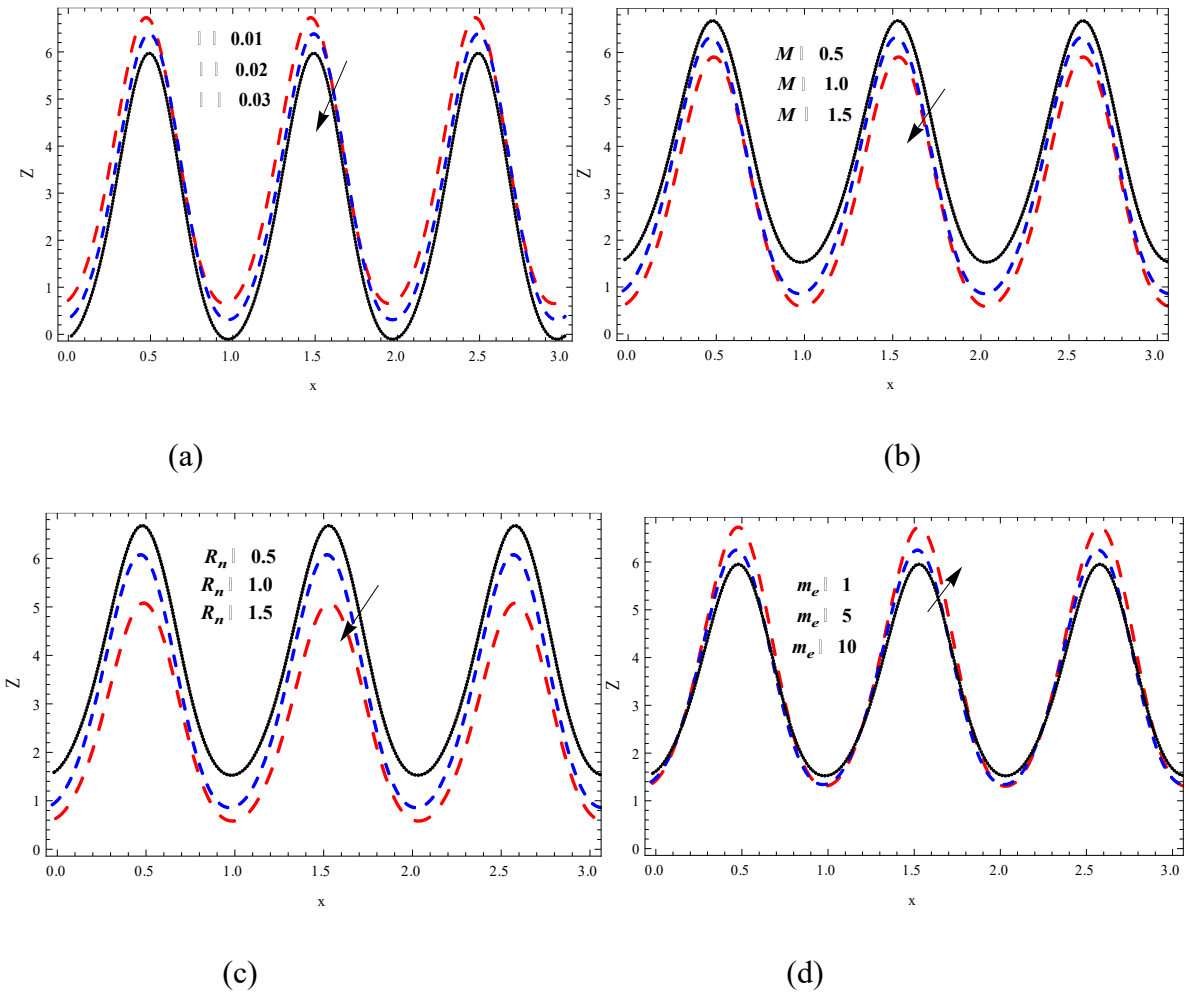

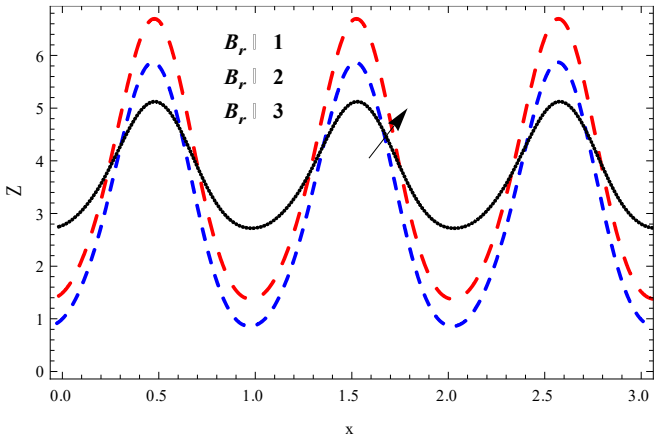


(e)

**Figure 5.** Heat transfer co-efficient ( $z$ ) for (a) $\Gamma$ (b) M (c) $R_n$ (d) $m_e$ (e) $B_r$, while other parameters are $x = 0.2, U = -2,\ m_e = 2, B_r = 2, \Gamma = 0.01, M = G_r = S_c = S_r = R_n = P_r = 0.5, G_c = 0.2, \Theta = 2$

Figure 5 illustrates the impact of heat transfer co-efficient Z for various values of Deborah number $\Gamma$ $(0 \leq \Gamma \leq 0.4)$, magnetic field parameter $M$ $(1 \leq M \leq 3)$, thermal radiation parameter $R_n$ $(0.0 \leq R_n \leq 0.6)$, electro-osmotic parameter $m_e$ $(1 \leq m_e \leq 10)$ and Brinkmann number $B_r$ $(1.0 \leq B_r \leq 3.0)$. Figure 5(a) shows that the heat transfer Z decreases with the increase in $\Gamma$ because the difference in temperature between a solid surface and surrounding fluid decreses for higher values of $\Gamma$ leading to a decrease in the heat transfer co-efficient. Similar behaviour is shown in the case of magnetic field parameter $M$ and thermal radiation parameter $R_n$ as depicted in Figure 5 (b) and (c) respectively. From Figure 4(d), it is observed that an increase in the electro-osmotic parameter $m_e$ enhances the mobility of the fluid particles, which increases the heat transfer rate. Figure 4(e) shows that the heat transfer coefficient rises with an increase in $B_r$. This is because Brinkmann number signifies the ratio of viscous heat generation to external heating. The higher its value, the slower the conduction of heat produced by viscous dissipation, and hence the larger the heat transfer co-efficient.

Comparison of the velocity profile ( $u$ ) for $m_e$, while other parameters are $x = 0.2, U = -2,\ m_e = 2, B_r = 2, \Gamma = 0.01, M = G_r = S_c = S_r = R_n = P_r = 1, G_c = 0.2, \Theta = 1.8.$

| y | Tanveer et al. [35] | Current work |
|---|---|---|
| -1.0 | -0.01158 | -0.01158 |
| -0.5 | -0.01675 | -0.01677 |
| 0.0 | -0.02195 | -0.02196 |
| 0.5 | -0.01157 | -0.01158 |
| 1.0 | -0.02714 | -0.02715 |

### 4.5. Trapping Phenomena

The streamlines are the imaginary lines in a fluid flow that provide us with the velocity at any location along the streamline. These lines will show the direction of movement of a zero-rest mass fluid element at any point in time. Trapping is the buildup of bolus of fluid in confined streamlines inside a wave frame. The nature of the streamlines against fluid parameter $\Gamma$ = 0.01, 0.02, 0.03, 0.04 respectively, is as shown in Figures 6. The fluid's viscosity relies on the parameter $\Gamma$, and it comes out to be highly viscous and turns thicker as we enhance the value of the third grade fluid parameter. Moreover, with the raising the values of the fluid parameter, the bolus will drastically shift to the middle of the channel, and the coupling streamlines slight below the wall.

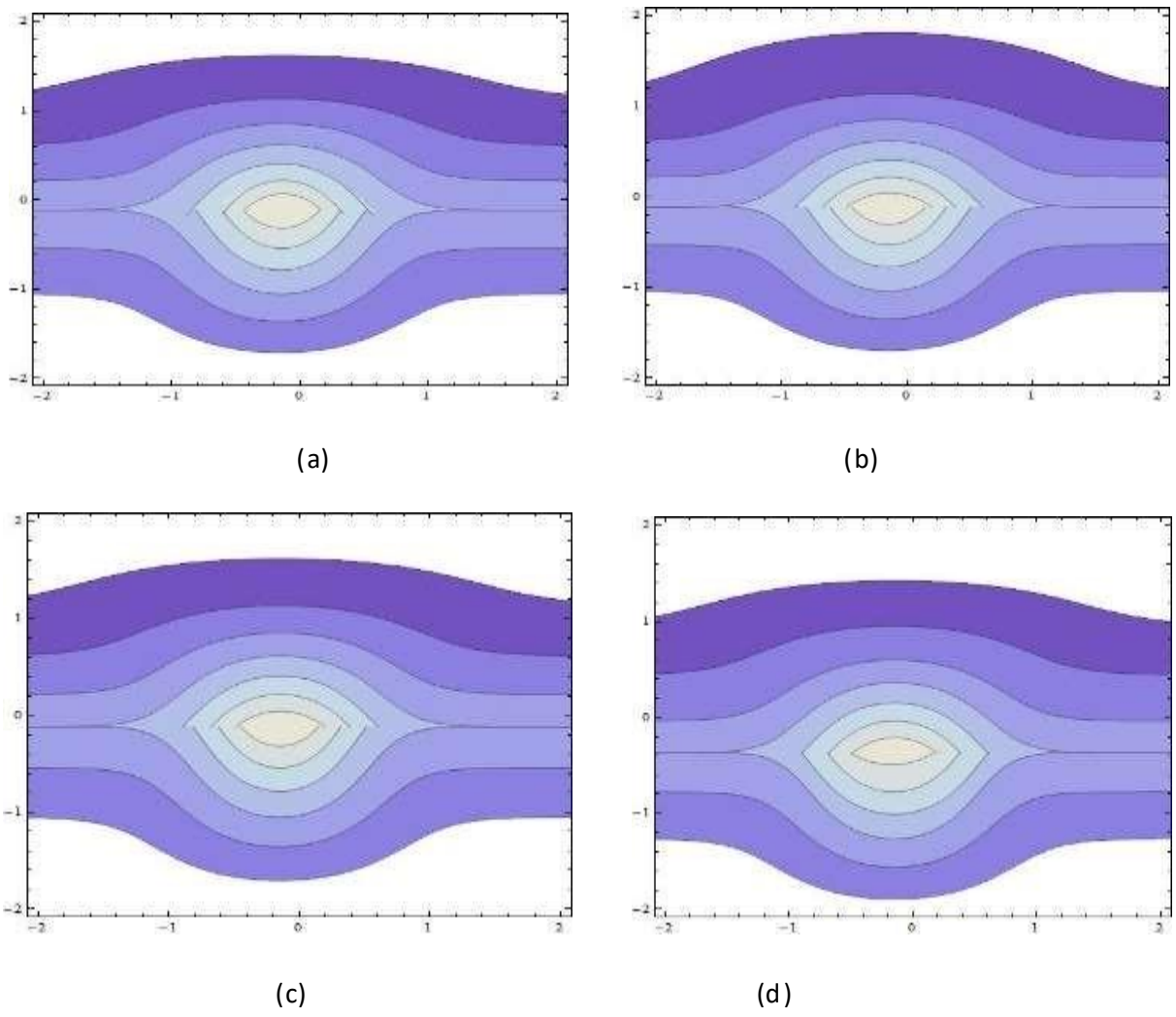


**Figure 6.** Streamline distribution (ψ) for (a) Γ =0.01 (b) Γ =0.02 (c) Γ =0.03 (d) Γ =0.04 while other parameters are $x = 0.2$, $U = -2$, $m_e = 2$, $B_r = 2$, $M = G_r = S_c = S_r = R_n = P_r = 0.5$, $G_c = 0.2$, $\Theta = 2$

## 5. CONCLUSIONS

In this paper, we explore the magneto-electrohydrodynamic peristaltic transport of a thirdgrade nanofluid flow in the presence of heat radiation in an asymmetric channel. Specifically, we focus on how the flow affects the magneto-electrohydrodynamic peristaltic transport. The effects of various physical parameters on the velocity, temperature, concentration of species, and heat transfer coefficient are explored and graphically examined. The following conclusions are drawn from this work:

- As the magnetic field parameter $M$ increases, the fluid's velocity decreases due to the Lorentz forces, which suppress the fluid motion.
- The magnitude of velocity enhances as the electroosmotic parameter $m_e$ increases. The magnitude of velocity for an asymmetric channel increases by 25% approximately, whereas for a symmetric channel increases by 95%.
- The Deborah number Γ raises the velocity profile in both symmetric and asymmetric channels. The velocity magnitude for an asymmetric channel increases by 20% approximately, whereas for a symmetric channel increases by 63%.
- Both thermal radiation parameter $R_n$ and heat transfer co-efficient Z have decreasing effect on temperature $\theta$.
- Brinkmann number $B_r$ causes the temperature to rise. This behaviour can be explained by greater thermal energy generated due to the viscous dissipation, which reduces the fluid temperature and concentration $\emptyset$ .
- Higher values of the Schmidt number $S_c$ and Soret number $S_r$ result in a decrease in concentration. Physically, increasing Sc means decreasing molecular diffusion, which diminishes the concentration.
- The fluid velocity in the channel increases close to the right wall and the left wall as the Grashoff number $G_r$ increases because the buoyant forces take precedence over the viscous forces.
- Deborah number Γ enhances the temperature profile, whereas it diminishes the concentration profile.
- An increase in the values of the fluid parameter Γ, the bolus will drastically shift to the middle of the channel, and the coupling streamlines slight below the wall.

**Declaration of Competing Interest**

The author declare that they have no known competing financial interests or personal relationships that could have appeared to influence the work reported in this paper.

**Funding Acknowledgement:** No

## Nomenclature:

$\phi$ Phase difference

$a_1$ Amplitude of the upper wall

$a_2$ Amplitude of the lower wall

$\tilde{t}$ Time

$\lambda$ Wavelength

$d_1$ Half-width of the upper wall

$d_2$ Half-width of the lower wall

$U$ Velocity in $X$ direction

$V$ Velocity in $Y$ direction

$\varepsilon$ Permittivity of dielectric

$\rho_e$ Overall density of charges

$\emptyset$ Electrical potential

e Electronic charge

$z_v$ Charge balance

$n_0$ Bulk concentration

$K_B$ Boltzmann constant

$T_{av}$ Average temperature

$m_e$ Electro-osmotic parameter

$T$ Stress tensor

$\tilde{I}$ Identity tensor

$p$ Pressure

$S$ Extra stress tensor

$\rho_e$ Electric charge density

$\rho$ Fluid density

$E_x$ Axial electric field

$P$ Pressure

$\sigma$ Electrical conductivity,

$k$ Thermal expansion coefficient,

g Acceleration due to gravity

$k'$ Concentration expansion co-efficient.

$q_r$ Radiated heat flux,

$k_t$ Thermal diffusion,

$D_m$ Mass diffusivity,

$T_m$ Average temperature

$\tilde{T}$ Non-dimensional temperature

$\tilde{C}$ Non-dimensional concentration

M Magnetic field parameter

$G_r$ Grashoff number

$G_c$ Species concentration Grashoff number

Γ Deborah number

$m_e$ Electro-osmotic parameter

$S_c$ Schmidt number

$S_r$ Soret number

$B_r$ Brinkmann number

$R_n$ Thermal radiation parameter

**References**

[1] Chakraborty, S. Augmentation of peristaltic microflows through electro-osmotic mechanisms. J. Phys. D Appl. Phys. (2006) 39, 5356.

[2] Abbasi A., Mabood F., Farooq W., Khan SU.Radiation and joule heating effects on electroosmosis-modulated peristaltic flow of Prandtl nanofluid via tapered channel Int Commun Heat Mass Transf, (2021) 123, 105183.

[3] Akram J., Akbar N S., Maraj EN. A comparative study on the role of nanoparticle dispersion in electroosmosis regulated peristaltic flow of water. Alex Eng J, 59 (2020), pp. 943-956

[4] Mabood F., Farooq W., AbbasiA .Entropy generation analysis in the electro-osmosis-modulated peristaltic flow of Eyring–Powell fluid. J Therm AnalCalorim (2021) 10.1007/s10973-021-10736-z.

[5] Jayavel P., Jhorar R., Tripathi D., Azese MN. Electroosmotic flow of pseudoplastic nanoliquids via peristaltic pumping. J Braz Soc Mech Sci, (2019) 41:61.

[6] D. Prasanth Reddy and M. V. Subba Reddy, "Peristaltic pumping of a third grade fluid in an asymmetric channel under the effect of magnetic field" Adv. Appl. Sci. Res, 3(6) (2012) 3868-3877.

[7] T. Hayat and O.U. Mehmood, "Slip effects on MHD flow of third order fluid in a planar channel" Comm nonlinear Sci Num Simulation, 16, (2011) 1363–1377.

[8] T.W. Latham, Fluid Motions in a Peristaltic Pump (M.S. Thesis) MIT, Cambridge, MA, (1996).

[9] A.H. Shapiro, M.Y. Jaffrey, S.L. Weinberg, Peristaltic pumping with long wavelengths at low Reynolds number, *J. Fluid Mech*. 37, pp.799-825 (1969).

[10] T. Hayat, F.M. Abbasi, A. Alsaedi, F. Alsaedi, Hall and Ohmic heating effects on the peristaltic Transport of Carreau-Yasuda fluid in an asymmetric channel, *Z. Naturforsch*., pp. 43-51 (2013).

[11] K.S. Mekheimer, Y.A. Elmaboud, A.I. Abdellateef, Peristaltic transport through eccentric Cylinders: Mathematical model, Appl. Bionics Biomech. 10, pp.19-27 (2013).

[12] T. Hayat, A. Tan veer, H. Yasmin, A. Alsaedi, Effects of convective conditions and chemical Reaction on peristaltic flow of Eyring-Powell fluid, Appl. Bionics Biomech.11, pp. 221-233 (2014).

[13] T. Hayat, H. Yasmin, B. Ahmad, B. Chen, Simultaneous effects of convective conditions and Nanoparticles on peristaltic motion. J. Mol. Liq. 193, pp. 74-82 (2014).

[14] M. Kothandapani and S. Srinivas, "Nonlinear peristaltic transport of a Newtonian fluid in an inclined asymmetric channel through a porous medium", Phys. Lett. A, 372 (2008) 1265-1276.

[15] V.P. Rathod and Laxmi Devindrappa, "Peristaltic transport in an inclined asymmetric channel with heat and mass transfer by Adomian decomposition method" Adv in Applied Sci and Research, 7 (2016) 83-100.

[16] K.K. Raju and R. Devanathan, Peristaltic motion of non-Newtonian fluids, Part-I, Rheol. Acta, 11 (1972) 170-178.

[17] Kh. S Mekheimer, "Peristaltic transport of blood under the effect of magnetic field in non-uniform channels, Appl. Math. Comput. 153 (2004) 763-777.

[18] C. Amrouche and D. Cioranescu, "On a class of fluids of grade 3", Internat. J. Non-Linear Mech, (1997) 73–88.

[19] V. Busuioc and D. Iftimie, "Global existence and uniqueness of solutions for the Eqs. of third grade fluids", Internat. J. Non-Linear Mech, 39 (2004) 1–12.

[20] D. Bresch and J. Lemoine, "On the existence of solutions for non-stationary third-grade fluids", Internat. J. Non-Linear Mech., 34 (1999).

[21] T. Hayat, Y. Wang, A.M. Siddiqui, K. Hutter and S. Asghar, "Peristaltic transport of a third order fluid in a circular cylindrical tube", Math. Models Methods Appl. Sci. 12 (2002) 1691-1706.

[22] M.H. Haroun, "Effect of Deborah number and phase difference on peristaltic transport of a third-order fluid in an asymmetric channel", Math. Comput. Modelling, 12, (2007) 1464–1480.

[23] J. Prakash, E.P. Siva, N. Balaji and M. Kothandapani, "Effect of peristaltic flow of a third grade fluid in a tapered asymmetric channel", Journal of Physics: Conf. Series. 1000 (2018) 012165.

[24] Amin, S. Islam, Taza Gul, M. Altaf Khan and S. Nasir, "Unsteady Thin Film Third Grade Fluid on a Vertical Oscillating Belt using Adomian Decomposition Method", J. Basic. Appl. Sci. Res, 4(8) (2014) 76-83.

[25] S. Sridhar, V.R. Babu, Heat and Mass Transfer Effect on Peristalsis of Jeffrey Fluid in a Vertical Channel with Thermal Radiation and Heat Sources, International Journal of Scientific and Innovative Mathematical Research (IJSIMR) 7 (2019) 18–32.

[26] J.E. Dunn and K. R. Rajagopal, "Fluids of differential type: Critical review and thermodynamic analysis", Int. J. Eng. Sci. 33 (5) (1995) 689-729.

[27] Y.S. Daniel, Z.A. Aziz, Z. Ismail, F. Salah, Entropy Analysis in Electrical Magnetohydrodynamic (MHD) Flow of Nanofluid with Effects of Thermal Radiation, Viscous Dissipation and Chemical reaction, Theoretical and Applied Mechanics Letters 7(2017) 235–242.

[28] T. Hayat, A. Bibi, H. Yasmin, F.E. Alsaadi, Magnetic field and thermal radiation effects in peristaltic flow with heat and mass convection, J. Therm. Sci. Eng. Appl. 10 (5) (2018).

[29] T. Hayat, R. Iqbal, A. Tanveer, A. Alsaedi, Influence of convective conditions in radiative peristaltic flow of pseudoplastic nanofluid in a tapered asymmetric channel, J. Magn. Magn. Mater. 408 (2016) 168–176.

[30] T. Hayat, M. Shafique, A. Tanveer, A. Alsaedi, Magnetohydrodynamic effects on peristaltic flow of hyperbolic tangent nanofluid with slip conditions and joule heating in an inclined channel, Int. J. Heat Mass Transf. 102(2016) 54–63.

[31] Asha, S. K., and C.K. Deepa. "Entropy Generation for Peristaltic Blood flow of a Magneto-micropolar Fuid with Thermal Radiation in a Tapered Asymmetric Channel." Results in Engineering (2019) 3(100024) doi:10.1016/j.rineng.2019.100024.

[32] Asha, S. K., and C.K. Deepa. "Influence of Induced Magnetic field and Heat Transfer on Peristaltic Blood flow of a Magneto-micro Polar fluid in a Tapered Asymmetric Channel." Heat Transfer-Asian Research (2019) 48:2714-2734. doi:10.1002/htj.21507.

[33] Asha, S. K., and C.K. Deepa. "Thermo-Diffusion and Diffusion-Thermo Effects on MHD Third Grade Nanofluid flow Driven by Peristaltic Transport." Arabian Journal for Science and Engineering (2020) 45:4995–5008 doi.org/10.1007/s13369-020-04590-8.

[34] Asha, S. K., and C.K. Deepa. "Bioconvective Peristaltic flow of a Third Grade Nanofluid Embodying Micro-organisms in the Presence of Cu-blood Nanoparticles with Permeable Walls." Multidiscipline Modelling in Materials and Structures (2021) 17: 293-316. doi.10.1108/MMMS-02-2020-0025.

[35] A. Tanveer, S. Mahmood,T. Hayat and A.Alsaedi, On electroosmosis in peristaltic activity of MHD non-Newtonian fluid, Alexandria Engineering Journal (2021) 60, 3369–3377.